Development of a WCMS Groundwater Modeling Component for Underground Mine Hydrologic Impact Assessment[1]

Robert N. Eli[2], Samuel J. Lamont, Jerald J. Fletcher, Thomas A. Galya

Abstract. The West Virginia Department of Environmental Protection (WVDEP) and the U.S. Office of Surface Mining, Reclamation and Enforcement (OSMRE) have identified a need for a groundwater modeling capability within the existing WCMS (Watershed Characterization and Modeling System). WCMS is a combination of software and data developed by the Natural Resource Analysis Center (NRAC) at West Virginia University (WVU). The software component of WCMS adds GIS tools to ESRI ArcGIS 9.x software to support the analysis of water quantity and quality issues throughout the state of West Virginia at a watershed scale consistent with the 1:24,000 scale NHD stream segmentation. WCMS is currently used by permit writers in the WVDEP Divisions of Water and Waste Management (DWWM) and Mining and Reclamation (DMR). The EPA HSPF (Hydrologic Simulation Program – Fortran) watershed model, a recent tool addition to WCMS, is accepted by state and federal agencies as one of the standards of surface water hydrology and water quality modeling. The WCMS-HSPF groundwater model component currently under development supports the use of MODFLOW as an option where adequate data are available and the additional analysis time can be justified. Although USGS MODFLOW is a universally accepted standard for groundwater modeling, MODFLOW applications are to be imbedded within a proposed spatially larger, more approximate WCMS routine, coined as the "Regional Groundwater Recharge Model" (RGRM), which effectively replaces the existing groundwater component within WCMS-HSPF. RGRM is to be calibrated jointly with HSPF using the recessionary portion of stream flow data, and will execute together with HSPF to close the groundwater mass balance portion of the watershed model. A new WCMS toolbar is being developed to support the addition of underground mine features and data input specific to the RGRM groundwater hydraulics.

Additional Key Words: MODFLOW, HSPF, GIS, RGRM

---

[1] Paper was presented at the 2008 "Incorporating Geospatial Technologies into SMCRA Business Processes", March 25 - 27, 2008, Atlanta, GA.

[2]Robert N. Eli is Associate Professor of Civil and Environmental Engineering, West Virginia University, Morgantown, WV 26506-6103

Samuel J. Lamont is Post Doctorial Scholar in the Natural Resource Analysis Center, West Virginia University, Morgantown, WV 26506-6108 http://www.nrac.wvu.edu

Jerald J. Fletcher is Professor and Director of the Natural Resource Analysis Center and the U.S. – China Energy Center, West Virginia University, Morgantown, WV 26506-6108 http://www.nrac.wvu.edu

Thomas A. Galya is Physical Scientist-Hydrology, U.S. Department of the Interior, Office of Surface Mining, 1027 Virginia St. East, Charleston, WV 25301

Introduction

The Natural Resources Analysis Center (NRAC) Watershed Characterization and Modeling System (WCMS) is an analysis tool widely used within the West Virginia Department of Environmental Protection (WVDEP) for a variety of applications related to water resource management (Fletcher, et al., 2004). Recently, WCMS capabilities were expanded with development of a new toolbar to support the application of the U.S. Environmental Protection Agency HSPF (Hydrologic Simulation Program-Fortran, Bicknell, et al., 2001) watershed hydrology and surface water quality model, which is a component of the EPA BASINS watershed management system (USEPA, 2001). WCMS provides specific GIS interface functionality that substantially automates the application of HSPF to mine-impacted watersheds, significantly reducing the complexity of watershed modeling analyses needed to evaluate new coal mine permit applications (Eli, et al., 2004, 2005). Additionally, a new model component has been developed to include the impacts of the proposed surface mine site hydrology, including the drainage plan design and NPDES (National Pollutant Discharge Elimination System) outflow points (Lamont, et al., 2005). Currently, WCMS-HSPF has been calibrated for use on 235 trend station watersheds within West Virginia by jointly calibrating five representative watersheds that share similar surface land use/vegetative cover, soils, topography, and geology with the trend station watersheds. Trend station watersheds have been defined by the WVDEP at stream locations where regular water quality monitoring is conducted.

WCMS-HSPF models the surface rainfall-runoff components of the hydrologic cycle. The subsurface is not explicitly modeled in HSPF, and therefore, the geologic structure and hydraulic characteristics of the subsurface, including the impacts of underground mines on the local and regional groundwater system, are not included. Conversely, the USGS MODFLOW groundwater model (Harbaugh, 2005) has been used to model the impacts of underground mining on groundwater systems (Sahu, 2003; Capo, 2004). MODFLOW is universally accepted as a standard for groundwater modeling as is HSPF for surface water modeling. The idea of combining the two to form a complete water basin modeling system is not new. The Integrated Hydrologic Model (IHM) is a combined HSPF-MODFLOW water basin modeling system developed for use in Florida where shallow water table aquifers predominate and hydraulic gradients are low (Ross, et al., 2004). Although this latter integrated system is impractical for

use in conjunction with WCMS in West Virginia due to differences in ground water regimes and data structures, joint use of HSPF and MODFLOW is a validated concept.

Development of a Regional Groundwater Recharge Model (RGRM) that is compatible with WCMS-HSPF and the underlying SLW (segment-level watershed) data structure of WCMS has been initiated to provide a more parsimonious solution to the groundwater modeling need in the coal mining areas of West Virginia. The development plan for the RGRM component supports the optional use MODFLOW as the primary underground mine site hydrologic model, imbedded within the much larger regional groundwater system modeled by RGRM. Since the RGRM component is to be run jointly with HSPF, and is also to be pre-calibrated to all trend station watersheds, it may be more accurately described as an extended HSPF capability rather than a separate groundwater modeling system. It will provide a broad-brush, approximate picture of the trend station watershed groundwater system opposed to that potentially provided by the more detailed modeling capabilities of MODFLOW.

The development of RGRM is in its first year of a three year design, development, and implementation project that will extend the current surface water modeling capability of WCMS into the groundwater domain. Year 1 will complete the design and testing of the basic model structure. Year 2 will add WCMS toolbars to implement the RGRM model functionality and its ability to represent underground mine cavities, mine pools, and vertical fracture impacts on aquifer dewatering and streamflow. Year 3 will complete verification testing, user training, and installation of the latest version of WCMS-HSPF-RGRM on the user network at WVDEP.

RGRM Model Structure

The WCMS GIS database will be expanded to include new spatial attribute data required for support of RGRM. WCMS maintains a statewide database of 1:24,000 scale NHD (National Hydrography Dataset) stream segments (reaches), and the associated DEM (30 m resolution, re-sampled to 20 m). Other existing data layers include land use/cover, surface drainage information, and the SLW (Segment Level Watershed) polygons associated with each NHD stream segment. A typical stream network example with the associated SLW's is illustrated in Figure 1 for the East Fork Twelve Pole Creek watershed (southwestern WV). The SLW's are

the highest resolution HRUs (Hydrologic Response Units) consistent with the NHD network, and are to be used as the primary level of spatial subdivision within the RGRM component.

Delaunay triangulation of the NHD SLW area centroids, as shown in Figure 2, establishes a network of connected points (nodes) from which Voronoi polygons (MATLAB, Mathworks, 2005) are constructed (Figure 3). The Delaunay triangulation establishes the spatial connectivity of the aquifer layers across the entire water basin being simulated via the triangulated irregular network (TIN) interconnections between nodes. The horizontal boundary of the control volume for maintaining the conservation of mass in each SLW aquifer layer corresponds to the actual boundary of that SLW and not the Voronoi polygon boundary. The Voronoi polygon sides are used to compute the directional flow cross section areas while the Delaunay triangle sides (links) are used to establish flow direction connectivity and to compute hydraulic gradients between adjacent SLWs. The connecting network of links is assumed to convey groundwater much the same way as pipes conveying water in a pipe flow network. The pipe network analogy allows a 2-dimensional model to be constructed using a one dimensional energy equation formulation (Darcy's law) within a set of algebraic equations that assure conservation of mass (groundwater) within each polygon. This approach, originally proposed by Narasimhan and Witherspoon (1976), significantly simplifies the solution for the SLW piezometric heads within each aquifer layer. It should be noted that the flow in the imaginary pipe network does not reflect the actual groundwater flow vector map. The groundwater flow vectors are generated in a post-processing step using the smoothed 3-dimensional piezometric surface for each aquifer layer.

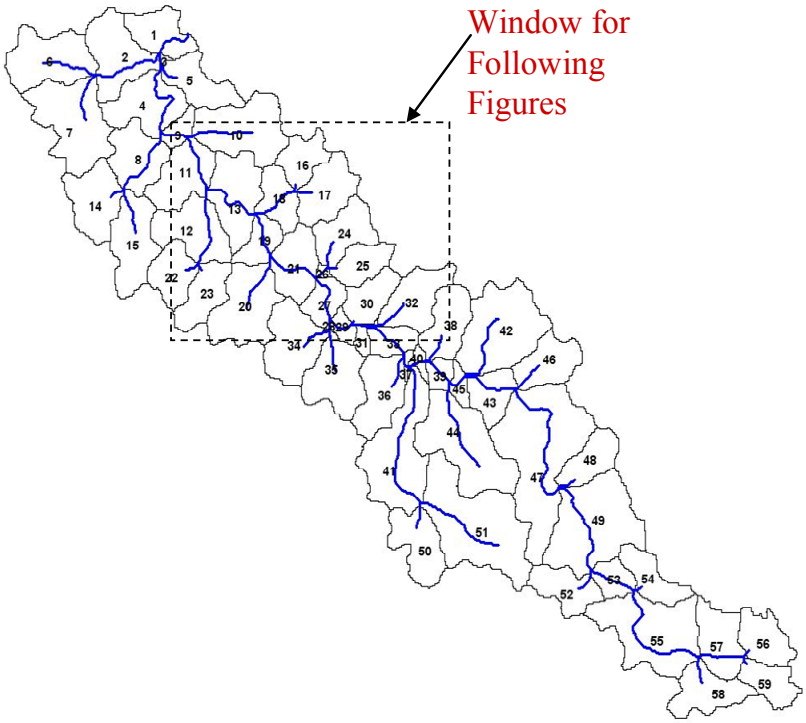

Figure 1. East Fork Twelve Pole Creek Stream Network and Associated Segment-Level Watersheds (SLW).

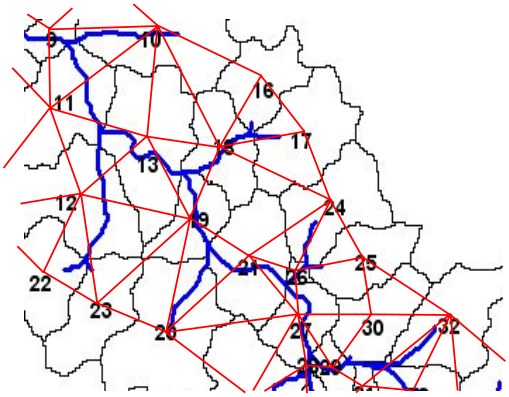

Figure 2. Delaunay Triangulation using the SLW Centroids.

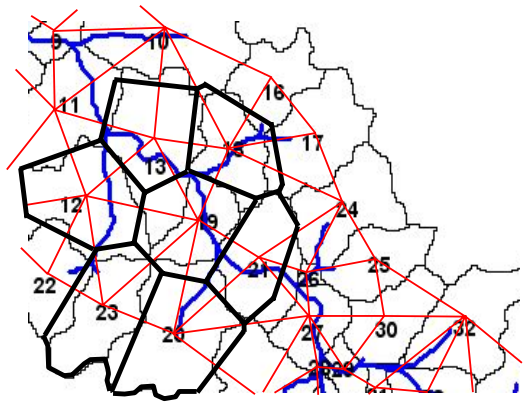

Figure 3. Voronoi Polygons Constructed Surrounding Segment-Level Watershed 19.

Single Layer Model

Initially, a single layer model was developed and tested with the flow assumed to be predominantly horizontal. Therefore a single equivalent horizontal hydraulic conductivity value was used for each flow direction and the aquifer was assumed to be unconfined with horizontal flow behavior according to the Dupuit assumption (Bear and Verruijt, 1987). The continuity equation is written for each connecting node (SLW centroid) in the Delaunay triangulation (Equation 1). Figure 4 illustrates the application of Equation 1 to a representative SLW.

$$\sum_j Q_{ij} - Q_i^* + I_i A_i^* = \frac{dS_i}{dt} = \frac{d\left(h_i A_i^* \eta_i\right)}{dt} = A_i^* \eta_i \frac{dh_i}{dt}$$

where:

$Q_{ij} =$ inflow to node i from adjacent node j $\left[m^3/d\right]$

$Q_i^* =$ outflow to SLW i stream segment $\left[m^3/d\right]$

$I_i =$ recharge rate in SLW i $\left[m/d\right]$ (1)

$A_i^* =$ SLW i planform area $\left[m^2\right]$

$S_i = h_i A_i^* \eta_i =$ SLW i groundwater storage volume $\left[m^3\right]$

$h_i =$ aquifer saturated thickness in SLW i $\left[m\right]$

$\eta_i =$ drainable porosity in SLW i

$t =$ time $\left[d\right]$

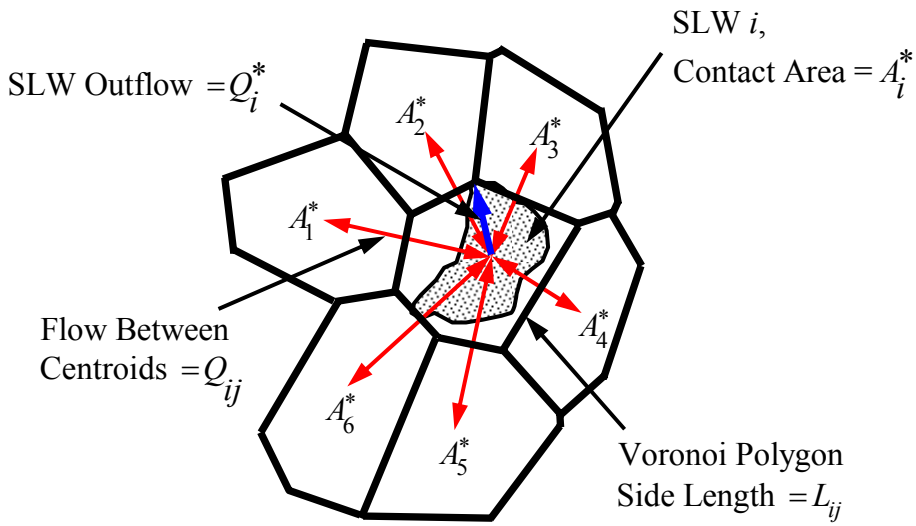

Figure 4. Groundwater flow exchange between the focus SLW and surrounding SLW's.

It should be noted that the summation sign convention in Equation 1 assumes that inflows to node i are positive and outflows are negative. Additionally, it is assumed that the drainable porosity η_i is equal to the specific yield as it is customarily defined in water table aquifers. The energy equation is written along each link (triangle side) of the Delaunay triangulation (Equation 2).

$$Q_{ij} = K_{ij} A_{ij} \frac{d\phi_{ij}}{dl_{ij}}$$

where:

$$\begin{aligned}
Q_{ij} &= \text{ flow from node } j \text{ to node } i \left[m^3/d \right] \\
K_{ij} &= \text{ hydraulic conductivity along link } ij \left[m/d \right] \\
A_{ij} &= \text{ flow cross section area along link } ij \left[m^2 \right] \\
\phi_{ij} &= \text{ piezometric level along link } ij \left[m \right] \\
\frac{d\phi_{ij}}{dl_{ij}} &= \text{ piezometric gradient from node } i \text{ to node } j \text{ along link } ij \\
l_{ij} &= \text{ link } ij \text{ length } \left[m \right]
\end{aligned} \tag{2}$$

The sign convention for the direction of flow Q_{ij} remains the same as in Equation 1. The flow cross section area A_{ij} is computed as a product of the Voronoi polygon side length L_{ij} bisecting link ij and the mean aquifer saturated thickness $\left(h_i + h_j\right)/2$ at that point. A special form of the energy equation is used to compute the outflow from SLW i to its stream segment Q_i^* (Equation 3).

$$Q_i^* = K_i^* A_i^* \frac{d\phi_i}{dl_i^*} \approx 2K_i^* \sqrt{A_i^*}\left(\phi_i - \phi_i^*\right)$$

where:

$\frac{d\phi_i}{dl_i^*}$ is approximated by $\frac{\left(\phi_i - \phi_i^*\right)}{\sqrt{A_i^*}/2}$

and where

$\phi_i^* =$ elevation of the outflow end of stream segment i $[m]$ (3)

$\phi_i =$ piezometric level in SLW i $[m]$

$l_i^* =$ flow length from centroid of SLW i to its outlet point $[m]$

$K_i^* =$ effective outflow hydraulic conductivity within SLW i $\left[m/d\right]$

$\sqrt{A_i^*}/2 =$ effective flow length from SLW i to its outlet point $[m]$

the remaining variables are defined as above

A backward in time finite difference equation can now be written for Equation 1 for each node i in the network (Equation 4).

$$\frac{\left(\sum_j Q_{ij} - Q_i^* + I_i A_i^*\right)^{t-\Delta t} + \left(\sum_j Q_{ij} - Q_i^* + I_i A_i^*\right)^{t}}{2} = A_i^* \eta_i \frac{\left(h_i\right)^t - \left(h_i\right)^{t-\Delta t}}{\Delta t} \tag{4}$$

Equation 2 can also be expressed in finite difference form along each link ij in the network (Equation 5).

$$\left(Q_{ij}\right)^{t} = K_{ij}\left(A_{ij}\right)^{t}\frac{\left(\phi_j - \phi_i\right)^{t}}{l_{ij}}$$

or

$$\left(Q_{ij}\right)^{t-\Delta t} = K_{ij}\left(A_{ij}\right)^{t-\Delta t}\frac{\left(\phi_j - \phi_i\right)^{t-\Delta t}}{l_{ij}} \tag{5}$$

where:

$$A_{ij} = \frac{h_i + h_j}{2}L_{ij}$$

$L_{ij} =$ Voronoi polygon side length bisecting link ij $[m]$

In Equation 5 it is important to note that if A_{ij} is evaluated at the same time step as the piezometric head ϕ, a nonlinear equation in the unknown piezometric head ϕ results at time step t. In the numerical procedure the nonlinear equation is avoided by using the flow area A_{ij} from the preceding time step. Substituting Equation 5 into Equation 4, and assuming that zero elevation datum corresponds to the aquifer bottom (then $h = \phi$), Equation 6 results.

$$\begin{aligned}
&\left[-\sum_j\left(\frac{K_{ij}\left(A_{ij}\right)^{t}}{2l_{ij}}\right) - K_i^*\sqrt{A_i^*} - \frac{A_i^*\eta_i}{\Delta t}\right]\left(\phi_i\right)^{t} + \sum_j\left(\frac{K_{ij}\left(A_{ij}\right)^{t}\left(\phi_j\right)^{t}}{2l_{ij}}\right) = \\
&\left[\sum_j\left(\frac{K_{ij}\left(A_{ij}\right)^{t-\Delta t}}{2l_{ij}}\right) + K_i^*\sqrt{A_i^*} - \frac{A_i^*\eta_i}{\Delta t}\right]\left(\phi_i\right)^{t-\Delta t} - \sum_j\left(\frac{K_{ij}\left(A_{ij}\right)^{t-\Delta t}\left(\phi_j\right)^{t-\Delta t}}{2l_{ij}}\right) \\
&-2K_i^*\sqrt{A_i^*}\phi_i^* - \left(\frac{\left(I_i\right)^{t-\Delta t} + \left(I_i\right)^{t}}{2}\right)A_i^*
\end{aligned} \tag{6}$$

The piezometric heads ϕ at time step t on the left hand side of Equation 6 are to be calculated as a function of the known quantities on the right side. Equation 6 is written for each SLW centroid (Delaunay triangle vertex) in the polygon network, yielding N equations in N unknown piezometric heads. Solution of the system of N equations is accomplished using matrix methods at each time step in the simulation. Following determination of the piezometric heads, connecting link flows and node outflows (to the stream segments) can be computed using Equations 3 and 5 for each time step.

Steady State Solution Verification

A steady state solution for the piezometric heads is often desired for a particular set of steady state boundary conditions (code verification in this case). This can be accomplished by simply running the unsteady simulation (using Equation 6) for a sufficient period of time steps for the solution to approach a steady state. However, this approach is inefficient since a large number of time steps will typically be required. The continuity equation (Equation 1) can be rewritten for the steady state solution, resulting in Equation 7.

$$\sum_j Q_{ij} - Q_i^* + I_i A_i^* = 0 \tag{7}$$

Equations 2 and 3 remain unchanged. Substituting Equations 2 and 3 into Equation 7 results in Equation 8.

$$\sum_j \left(K_{ij} A_{ij} \frac{d\phi_{ij}}{dl_{ij}} \right) - K_i^* A_i^* \frac{d\phi_i}{dl_i^*} + I_i A_i^* = 0 \tag{8}$$

A finite difference form of Equation 8 can be written using the iteration index n (Equation 9).

$$\sum \left(K_{ij} \left(A_{ij} \right)_{n-1} \frac{\left(\phi_j - \phi_i \right)_n}{l_{ij}} \right) - K_i^* A_i^* \frac{\left(\phi_i - \phi_i^* \right)_n}{\sqrt{A_i^*}/2} + I_i A_i^* = 0$$

where (9)

$$A_{ij} = \frac{h_i + h_j}{2} L_{ij}$$

Equation 9 can be expanded to a form more convenient for writing N linear equations in N unknown piezometric heads at iteration n (Equation 10).

$$\left[-\sum_j\left(\frac{K_{ij}\left(A_{ij}\right)_{n-1}}{l_{ij}}\right)-2K_i^*\sqrt{A_i^*}\right]\left(\phi_i\right)_n+\sum_j\left(\frac{K_{ij}\left(A_{ij}\right)_{n-1}\left(\phi_j\right)_n}{l_{ij}}\right)=-2K_i^*\sqrt{A_i^*}\phi_i^*-I_iA_i^*$$

where (10)

$$A_{ij}=\frac{h_i+h_j}{2}L_{ij}$$

Equation 10 can be solved directly for the piezometric heads ϕ at iteration n using the aquifer saturated thickness h computed from the previous iteration n-1. The aquifer saturated thickness is then updated with the current computed value and the piezometric heads recomputed. Approximately 5 iterations are required for convergence.

Steady State Verification – Flow Between Two Reservoirs

Equation 10 was implemented in MATLAB code (MATLAB, 2005) for the case of steady unconfined flow between two reservoirs. Since a square grid of node points define Voronoi polygons that are squares, this configuration (see Figure 5) was selected as best suited for this one-dimensional flow problem. The analytical solution for the saturated flow thickness h is Equation 11 (Bear, 1972, pgs 366-367) which uses the Dupuit approximation (horizontal flow only).

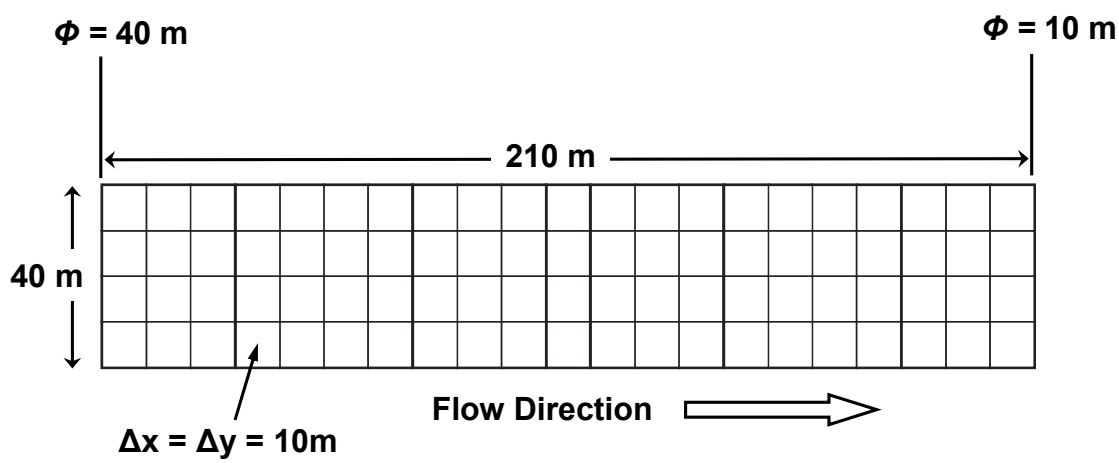

Figure 5. Square computational grid used for steady-state solution verification.

$$h_x = \sqrt{h_{x=0}^2 - 2Qx/K}$$

where

$h_x =$ saturated flow thickness at distance $0 \le x \le L$ $[m]$

$Q =$ total discharge per unit width $\left[m^2/d\right]$ (11)

$$= \frac{K\left(h_{x=0}^2 - h_{x=L}^2\right)}{2L}$$

$K =$ hydraulic conductivity $[m/d]$

In this example the left reservoir ($x = 0$) has a depth of 40 m and the right reservoir ($x = L$) has a depth of 10 m, where $L = 210$ m. A square grid of 22 nodes was spaced at $\Delta x = 10$ m over the 210 m length (Figure 6). The width of the grid was limited to 4 nodes since the flow is entirely one-dimensional in the x-direction. The hydraulic conductivity was set constant at 1 m/day. The computed solution for the 20 interior nodes (inside the left and right boundary conditions) after 5 iterations was essentially identical to that predicted by Equation 11. The RMS error of the computed head values = 1.3796e^{-6} m.

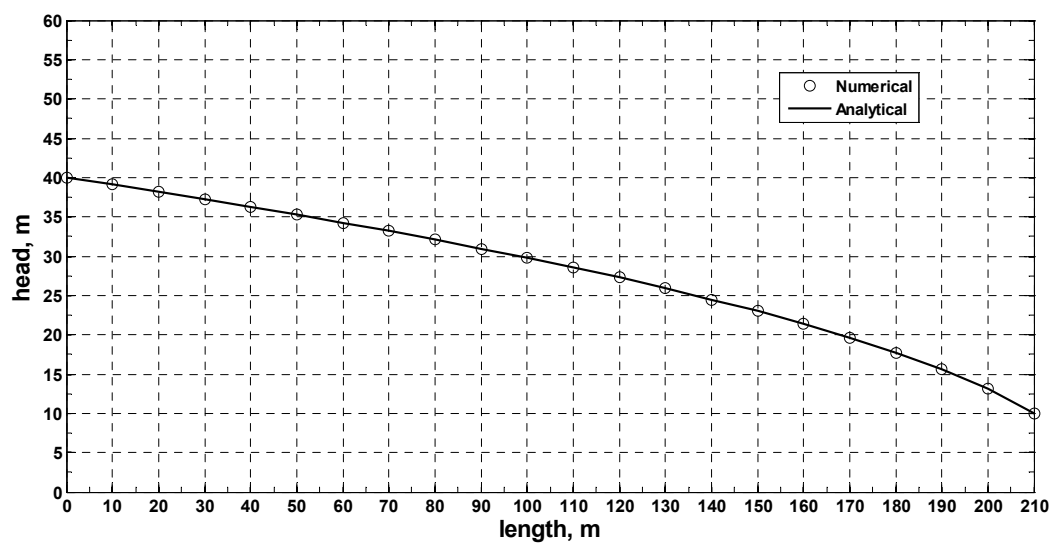

Figure 6. Comparison of steady state numerical solution to analytical solution for unconfined flow between two reservoirs.

Unsteady Flow Solution Verification

Following verification of the steady state solution, Equation 6 (the unsteady finite difference equation) was coded in MATLAB for testing against the same two reservoir case above using the same grid dimensions (Figure 5). But unlike the steady state solution, cyclic boundary conditions were imposed in the grid direction normal to the direction of flow. Since the grid has four columns (nodes) in the normal direction, the first column of nodes and the fourth column of nodes must be connected with a flow link normal to the flow direction (along the grid rows). In terms of grid geometry, this is analogous to rolling the grid into a cylinder so that the first and fourth columns of the grid can be connected together. Cyclic conditions are required to properly simulate a one dimensional flow in the vertical plane since, mathematically, the flow is assumed to extend infinitely into and out of the plane of the paper.

The verification test consisted of starting the simulation with initial conditions shown in Figure 7 at t = 0. All interior grid nodes were initialized to a head of 40 m (same as the fixed reservoir head on the left) except for the last grid row on the right which corresponded to the fixed 10 m reservoir head. The hydraulic conductivity remained the same (1 m/day) and the drainable porosity η (equal to the specific yield S) was set equal to 0.2. The solution was computed for variable times and time increments to explore the solution characteristics. A time increment of 1 day was found to produce divergent errors (instability). A time increment of 0.1 day was found to give good results (it is noted that a later computer code correction eliminated the instability problem when using daily time increments). A total simulation time of about 2000 days (20,000 time steps) was required for the numerical solution to approach the steady state analytical solution. As shown in Figure 7 the numerical solution at this point in time was indistinguishable from the analytical solution. When Equation 6 is solved for the collapse of the piezometric surface to a steady state, as shown in Figure 7, the saturated thickness between nodes will approach the correct value as the transient solution converges to the steady state solution.

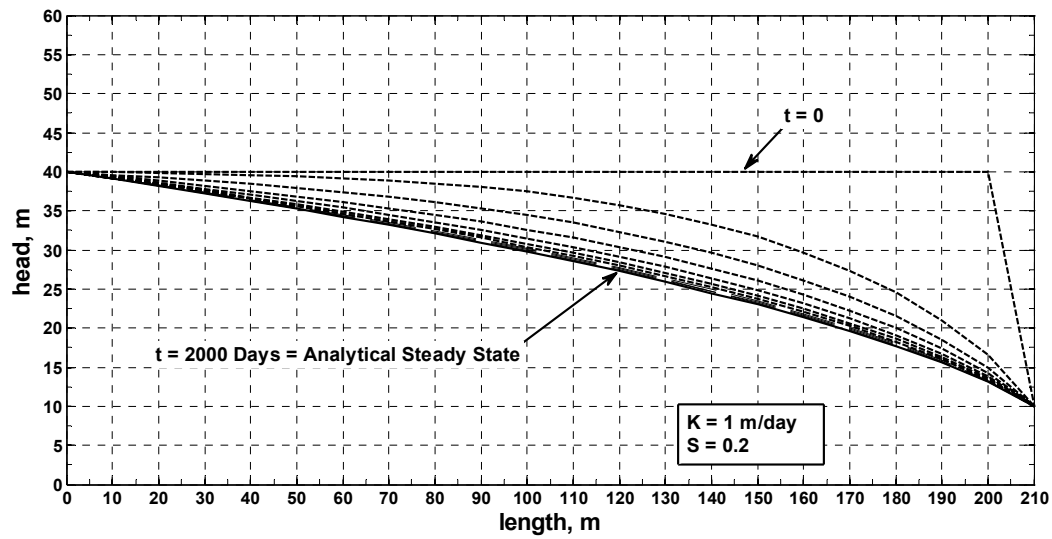

Figure 7. Unsteady flow numerical solution: from horizontal water table to the steady state analytical solution shown in Figure 6 (plotted at Δt = 200 days).

The next unsteady flow verification test used a time-dependent analytical solution consisting of a declining piezometric surface between to parallel drains (Bear, 1972, pgs 381-383). Equation 12 is the analytical solution which uses the Dupuit approximation.

$$h(x,t) = \frac{h_0(x)}{\left[1 + \beta K h_0(L) \big/ \left(\eta L^2 t\right)\right]}$$

where

$$h_0(x) = h_0(L) F(x/L)$$

$$F(x/L) = \left(1.321 - 0.142\left(x/L\right) - 0.179\left(x/L\right)^2\right)\sqrt{\left(x/L\right)} \tag{12}$$

$$\beta = 1.12$$

$K =$ hydraulic conductivity

$\eta =$ drainable porosity

$t =$ time

As shown in Figure 8, the x axis origin is at the left drain location and extends to the axis of symmetry where $x = L$. The opposite side (extending on to the right drain) is a mirror image of the left side of the solution domain. The solution at $t = 0$ is solved first by selecting a value of $h_0(L)$ and solving for the corresponding head values $h_0(x)$ using lower portion of Equation 12. The solution for heads $h(x,t)$ can then be computed using the top relationship in Equation 12 at

any desired time t. The analytical solution and numerical model are set up for $L = 210$ m and $h_0(L) = 40$ m, therefore there are 43 grid rows (nodes) spaced at 10 m in the numerical model (see Figure 8). As before (referring to Figure 5), there are four columns (four nodes in width) in the numerical grid. Again, cyclic boundary conditions are used, linking column one to column four. The simulation was run for a total of 500 days using daily time increments. As shown in Figure 9, the numerical solution (points) show excellent agreement with the analytical solution (lines) given by Equation 12. The RMS errors are listed in Table 1.

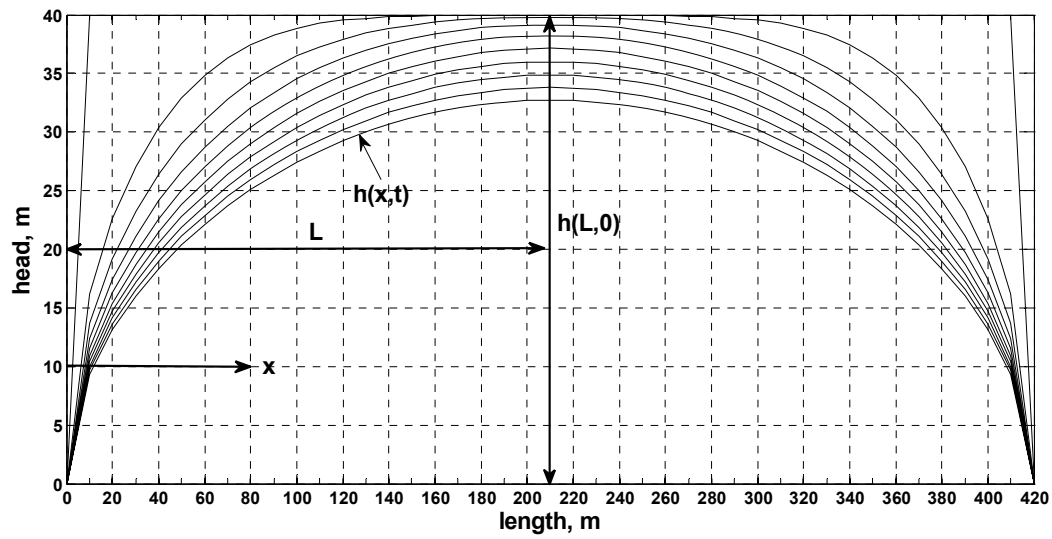

Figure 8. Declining piezometric head between parallel drains: analytical solution domain variables.

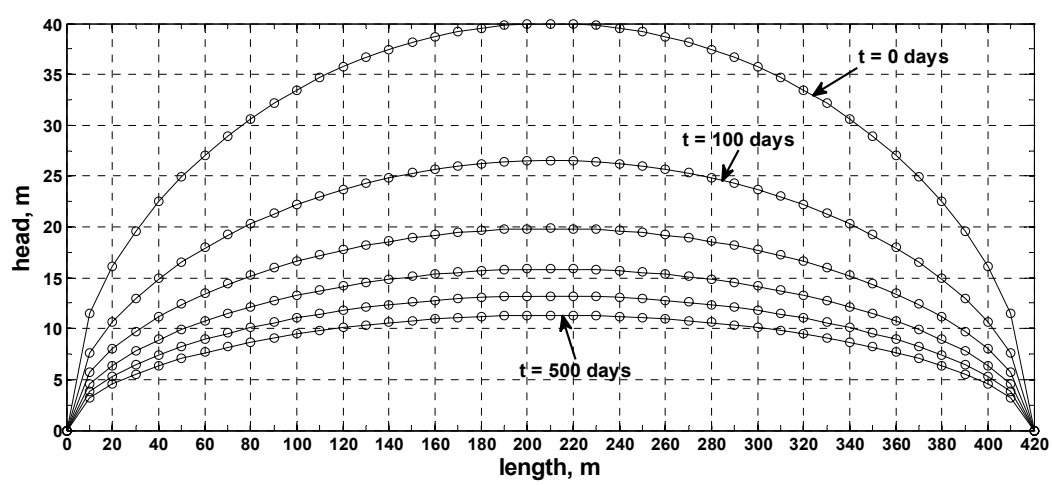

Figure 9. Declining piezometric head between parallel drains: numerical solution (points) versus analytical solution (lines).

Table 1. RMS error results for the numerical solution shown in Figure 9.

Time, Days	rms error, m
100	0.024892
200	0.027767
300	0.027570
400	0.026344
500	0.024836

Model Extensions: Quasi-3-Dimensional Flow

As shown in Figures 3 and 4, the groundwater domain is subdivided into Voronoi polygons in the horizontal plane at a scale consistent with the Segment Level Watersheds (SLW) contained in the WCMS database. At the 1:24,000 scale of the NHD (National Hydrography Dataset), SLW areas average approximately 60 ha (150 acres). As shown in Figure 10, additional horizontal resolution to represent underground mine cavities or other small features such as fault lines and fractures can be achieved by adding additional local control points to control size and location of the Voronoi polygons they create, and the flow directions between the polygon centroids.

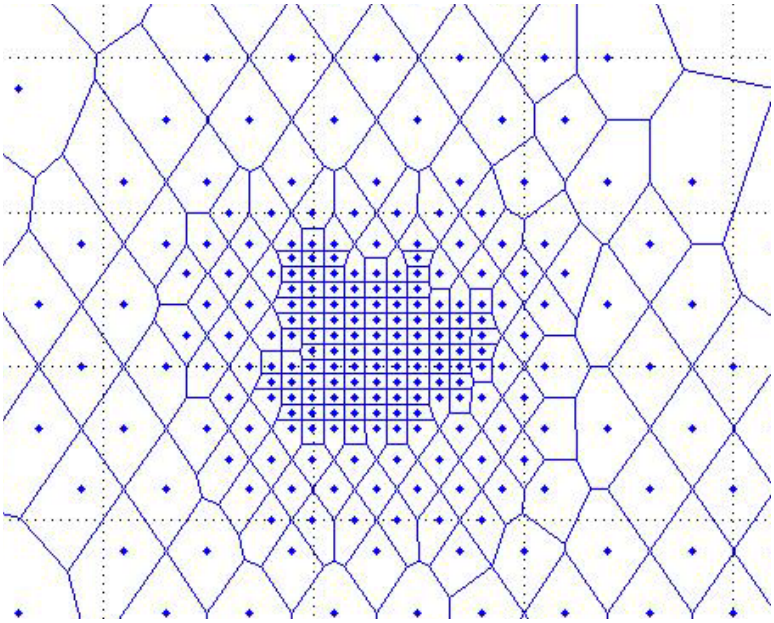

Figure 10. Additional control points define local subsurface features such as mines.

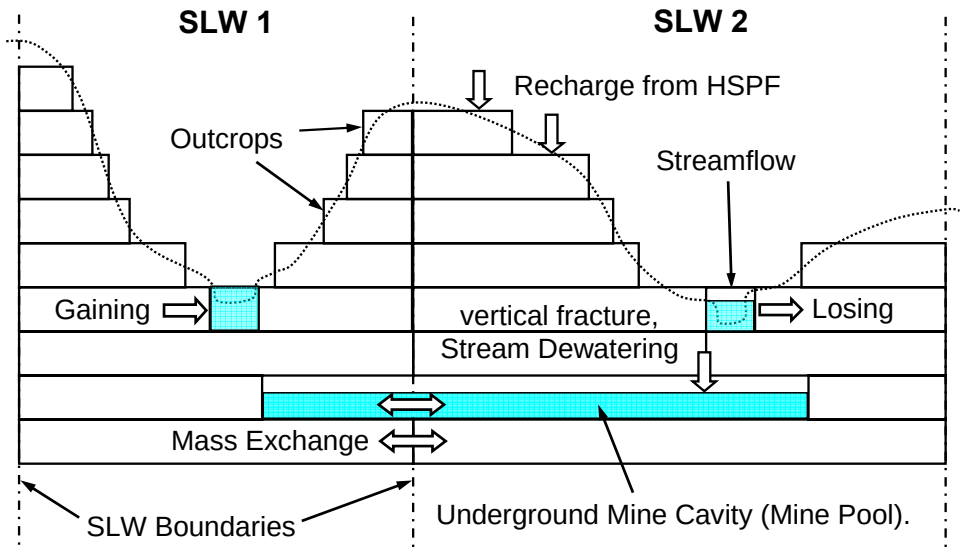

Figure 11. Schematic of important hydrogeology features to be represented in RGRM.

As illustrated in Figure 11, a single layer model structure cannot represent the multi-layered subsurface structure typical of sedimentary basins. In order to include such features as perched water tables, stream and aquifer dewatering due to fractures, and the accumulation of mine pools, RGRM must have some ability to account for a vertical component of groundwater flow and its storage in layered geologic strata. RGRM is currently being modified to include multiple aquifer layers separated by thin confining layers, as shown in Figure 12. Since RGRM is intended to be significantly simpler to apply as compared to MODFLOW, maintaining a 2-dimensional model structure is important. The structure shown in Figure 12 can be described as a quasi-3-dimensional model of groundwater flow. Specifically, a 2-dimensional solution scheme includes features that allow vertical flow between the layers that is controlled by a thin confining layer that has a specified resistance to vertical flow, thus permitting anisotropic aquifer characteristics to be simulated.

As shown in Figure 12, a layered model structure can approximate layers of consolidated sediments typical of coal fields throughout the country. Dip in strata can be approximated by introducing elevation offsets as illustrated in Figure 13. The abrupt discontinuity shown at the SLW boundaries represents the boundary separation in layer storage volumes and does not influence the groundwater hydraulics between layer segments since the connecting links between SLW centroids within each layer are lines that have continuous slopes that are consistent with the drop in elevation. It should be noted that the algorithm proposed for the quasi-3-dimensional

version of RGRM will permit layers to change thickness, or to terminate at the SLW boundaries, in addition to elevation changes.

Equation 1 can be modified for application to the layered structure shown in Figure 12. Equation 13 illustrates the proposed form of the continuity equation (conservation of mass) written for the center layer shown in Figure 12. Vertical flow between adjacent layers is added to the lateral flow between adjacent SLW's to balance the flow into and out of that layer. A layer can potentially be dewatered, which would add a storage term to the right side of Equation 13. A minimum of three layers (as shown in Figure 12), with no specified maximum number, will be supported in the model. The top layer will require additional terms to be added to Equation 13 to accept percolation inflow from the surface water mode (HSPF), and to allow outflow to each stream segment that is associated with each SLW. Equation 13 (with modifications appropriate for the top layer, and to permit dewatering) is written for each layer in a given SLW, yielding a set of equations that can be solved simultaneously for the piezometric levels in each layer. Hydraulic gradients between the focus SLW and adjacent SLW's are initially estimated using the piezometric levels computed in the previous time step. The piezometric levels are then converged to the true values using Gauss-Seidel iteration (Pozrikidis (1998)).

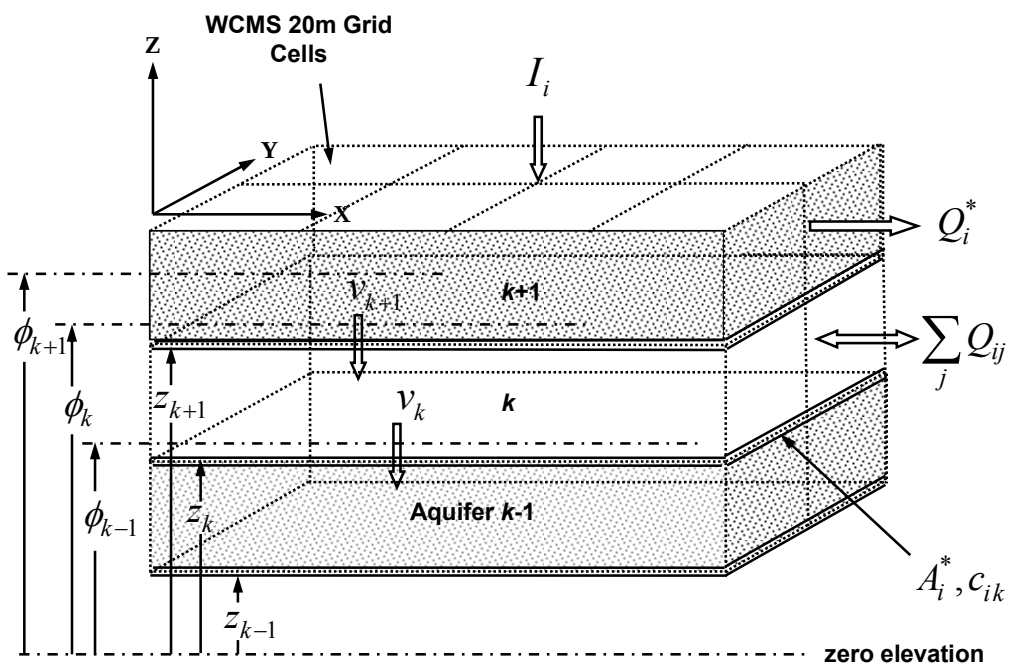

Figure 12. Modeling of anisotropic properties using alternating aquifer and confining layers.

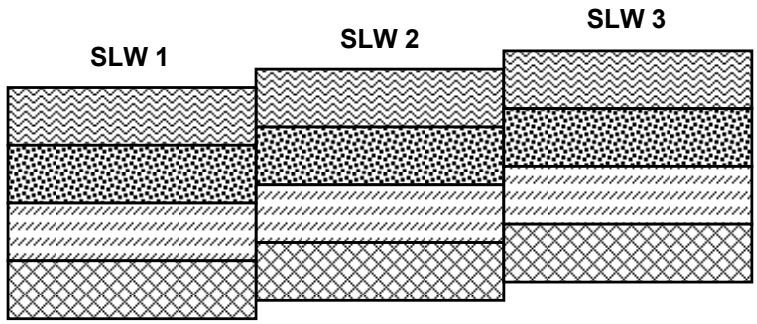

Figure 13. Approximation of dip in geologic strata using SLW layer elevation offsets.

$$\sum_j Q_{ij} - v_k A_i^* + v_{k+1} A_i^* = 0$$

where:

$Q_{ij} =$ inflow to node i from adjacent node j $\left[m^3 / d \right]$

$A_i^* =$ SLW i planform area $\left[m^2 \right]$

$v_k =$ aquifer leakage through bottom per unit area $\left[m / day \right]$

$v_{k+1} =$ aquifer leakage through top per unit area $\left[m / day \right]$

the aquifer leakage terms are conditional:

$$v_k = \frac{\phi_k - \phi_{k-1}}{c_k} \qquad \left\{ \phi_k \geq z_k, \phi_{k-1} \geq z_k \right\}$$

$$v_k = \frac{\phi_k - z_k}{c_k} \qquad \left\{ \phi_k \geq z_k, \phi_{k-1} \leq z_k \right\}$$

$$v_{k+1} = \frac{\phi_{k+1} - \phi_k}{c_{k+1}} \qquad \left\{ \phi_{k+1} \geq z_{k+1}, \phi_k \geq z_{k+1} \right\}$$

$$v_{k+1} = \frac{\phi_{k+1} - z_{k+1}}{c_{k+1}} \qquad \left\{ \phi_{k+1} \geq z_{k+1}, \phi_k \leq z_{k+1} \right\} \tag{13}$$

where:

$\phi_k =$ piezometric level $\left[m \right]$

$c_k = \dfrac{b_k}{K_k^*}$ -- resistance of the confining layer $\left[day \right]$

$b_k =$ confining layer thickness $\left[m \right]$

$K_k^* =$ vertical hydraulic conductivity of confining layer $\left[m / day \right]$

Summary and Conclusions

The HSPF model is continuous simulation watershed model that includes all of the principal components of surface and subsurface hydrologic processes (Bicknell, et al, 2001). It focuses on the surface and soil water processes, but includes a simple groundwater component to permit closure of the surface water hydrologic balance via outflow to the stream reach, or by allocation to inactive groundwater storage. The groundwater component is a simple reservoir-recessionary flow model that is associated with each land use – land cover category for which a single HSPF PERLND (pervious land segment) component is defined. Therefore, the HSPF groundwater component operates independently within each individual PERLND and does not reflect any connectivity with the other groundwater components in adjacent PERLND's, and bears no resemblance to the reality of spatial interconnectivity of groundwater systems found in a typical drainage basin. RGRM is intended to correct this shortcoming within HSPF. The inflow to the groundwater reservoir in HSPF can be output as a time series for the simulation period and applied as input to the RGRM model as the recharge rate I_i (see Figure 12). After running RGRM for the same simulation time period, the corrected groundwater outflow time series then replaces that generated by HSPF. Some limited recalibration of HSPF may be required to adjust the recharge rate to reflect the correct mass balance for the simulated watershed. This correction should better reflect the spatial distribution of dry weather recessionary stream flows within the watershed stream network.

Currently, the RGRM single aquifer layer modeling concept presented above has been developed and tested. The single layer model is currently being modified to include multiple layers with a vertical flow capability that will ultimately transform it to a quasi-3-dimensional groundwater model. RGRM's principal task is to improve simulation of spatially and temporally distributed groundwater recharge rates, outflows to streams, and interception of groundwater by existing and proposed underground coal mines. This capability is intended to support the assessment of mining impacts on the groundwater and surface water mass balance within the affected drainage basin at a level of accuracy and representation consistent with the limited availability data. RGRM is being designed to be strongly mass conservative, and is intended to be calibrated jointly with HSPF by comparing the groundwater component supplied to streamflow to that obtained from stream gage data (or available statistical low flow data). The

primary hydraulic parameters to be used in calibration are aquifer hydraulic conductivity, confining layer resistance, and specific storage. Future work includes completion of the multiple layer option and the development of user interface tools for addition of mine cavities and fracture flow paths for simulation of mine subsidence impacts on stream flow.

Acknowledgements

The authors express their appreciation for the support of the West Virginia Department of Environmental Protection and the U.S. Dept. of Interior Office of Surface Mining, Reclamation and Enforcement, under the Applied Science Cooperative Agreement Program, Cooperative Agreement Number S07AZ12498.

Literature Cited

Bicknell, B.R. et al. 2001. Hydrological Simulation Program - Fortran, HSPF Version 12 User's Manual. U.S. EPA. Athens, Georgia.

Bear, Jacob 1972. Dynamics of Fluids in Porous Media. Environmental Science Series. American Elsevier Publishing Co., Inc. New York.

Bear, Jacob, and Verruijt, Arnold; 1987. Modeling Groundwater Flow and Pollution. D. Reidel Publishing Company. Boston, Mass.

Capo, Rosemary C., 2004. Evolution of Historically Acidic Mine Drainage (AMD) to Alkaline Discharges: Irwin Coal Basin, Pennsylvania. 2004 Denver Annual Meeting. Geological Society of America. Paper No. 99-5. Denver, CO. November 7-10.

Eli, Robert N.; Fletcher, Jerald J.; Galya, Thomas A.; Strager, Michael P.; Lamont, Samuel J.; Sun, Quingyun; Churchill, John B.; 2004. Hydrologic Modeling Tools for Cumulative Hydrologic Impact Assessment of West Virginia Coal Mine Permits. Advanced Integration of Geospatial Technologies in Mining and Reclamation. US Dept. of Interior Office of Surface Mining. Atlanta, Georgia. December 7-9.

Eli, Robert N.; Fletcher, Jerald J.; 2005. Cumulative Hydrologic Impact Assessment of West Virginia Coal Mine Permits Using HSPF and WCMS. Watershed Management Conference

2005: Managing Watersheds for Human and Natural Impacts, Engineering, Ecological, and Economic Challenges. American Society of Civil Engineers. Williamsburg, Virginia. July 19-22.

Fletcher, Jerald J.; Eli, Robert N.; Galya, Thomas A.; Strager, Michael P.; Lamont, Samuel J.; Sun, Quingyun; Churchill, John B.; Schaer, Andrew N.; 2004. The Watershed Characterization and Modeling System (WCMS): Support Tools for Large Watershed CHIA and NPDES Analyses. Advanced Integration of Geospatial Technologies in Mining and Reclamation. US Dept. of Interior Office of Surface Mining. Atlanta, Georgia, December 7-9.

Harbaugh, A.W., 2005, MODFLOW-2005, The U.S. Geological Survey Modular Ground-Water Model—The Groundwater Flow Process. U.S. Geological Survey Techniques and Methods 6-A16.

Lamont, Samuel; Eli, Robert; Fletcher, Jerald J.; 2005. The Calibration of a Complex Watershed Model in Sparse Data Environments – Use of Supplemental Indices. Watershed Management Conference 2005: Managing Watersheds for Human and Natural Impacts. Engineering, Ecological, and Economic Challenges. American Society of Civil Engineers. Williamsburg, Virginia. July 19-22.

MATLAB, Version 7, 2005. The Mathworks, Inc. www.mathworks.com.

Narasimhan, T.N. and Witherspoon, P.A. 1976. An Integrated Finite Difference Method for Analyzing Fluid Flow in a Porous Media. Water Resources Research. 12, pgs. 57-64.

Pozrikidis, C. 1998. Numerical Computation in Science and Engineering. Oxford University Press, New York, N.Y.

Ross, Mark; Geurink, Jeffrey; Aly, Alaa; Tara, Patrick; Trout, Ken; and Jobes, Tom; 2004. Integrated Hydrologic Model (IHM), Volume I: Theory Manual. Intera Inc., University of South Florida. Aqua Terra Consultants.

Sahu, Parameswar, 2003. Modeling Groundwater Flow in Abandoned Underground Coal Mines of the Corning Mine Complex, Perry County, Ohio. 2003 Seattle Annual Meeting. Geological Society of America. Paper No. 252-4. Seattle, WA. Nov. 2-5.

USEPA, 2001. User's Manual: Better Assessment Science Integrating Point and Nonpoint Sources: BASINS Version 3.0, EPA-823-B-01-001, U.S. Environmental Protection Agency, Washington, D.C.